Channel Modeling for Multiple Satellite Broadcasting Systems

Marko Milojević, *Student Member, IEEE*, Martin Haardt, *Senior Member, IEEE*, Ernst Eberlein, and Albert Heuberger, *Member, IEEE*

***Abstract*—In this contribution we present the results of a study on land mobile satellite channel models for satellite systems with multiple satellites. The slow fading of our channel model for several satellites is based on a Markov channel state model for joint processes while the Probability Density Function (PDF) of the signal amplitude within each state is fitted to the Loo distribution. The correlation between two satellite channels and the channel spatial autocorrelation have also been studied. We show that a channel state model that uses a Markov state model of order one or of a fixed higher order is not appropriate if the state duration is of very high importance, which can be the case in the process of system planning. Therefore, we propose a dynamic higher order Markov state model for joint processes that depends on the current state duration. This approach models precisely any PDF of the channel state duration for both single and multiple satellite broadcasting systems while having a significantly lower computational complexity than a fixed higher order Markov model. It models the channel states of the whole system correctly, as well as the channel states of each satellite observed independently. It is able to capture the state correlation between multiple satellites. We also study possible approximations of the proposed models in order to reduce their computational complexity while having a good PDF match. Our channel state models are validated by measurements.**

***Index Terms*—Channel modeling, Markov processes, multiple satellite systems, satellite broadcasting.**

I. Introduction

SATELLITE broadcasting systems allow the coverage of large areas. The usage of two or more simultaneously transmitting satellites as in, for example, XM Radio or Sirius systems, improves the broadcasting reception. Such systems can capture time, spatial, and frequency diversity. The characterization of the propagation environment is of the highest importance for the system planning. Usually Land Mobile Satellite (LMS) channels are modeled with two processes. The first process models the slow fading by introducing a Markov channel state model concept, while the second process models the signal amplitude statistics. The latter process is studied in many contributions and is characterized by various combinations of Ricean, Rayleigh, and log-normal PDFs. The difference between the models is in the interpretation of the shadowing mechanism for direct and scattered paths. In [1] a linear combination of log-normal, Rayleigh, and Rice models is used to describe the signal amplitude and phase variations on shadowed satellite channels. In [2] it is assumed that the amplitude of the Line-Of-Sight (LOS) component after shadowing is log-normally distributed and that the received multi-path contribution has a Rayleigh distribution. A new shadowed Rice model that shows a similar performance as Loo's model [2)] has been proposed in [3]. The Suzuki distribution has been introduced in [4]. Based on extensive measurements and on the physical phenomena of multi-path fading and signal shadowing, a statistical model of the LMS channel is introduced in [5]. Starting from the two-state Markov models for two separate LMS channels, a combined model for two channels is developed in [6]. The parameters of the model are analytically derived. In [7]–[9] a statistical model capable of describing both narrow-band and wide-band conditions for a set of environments and satellite elevations is presented: the parameters of a three state Markov channel model are extracted from measurements in S-band and fitted to the proposed Loo distribution of the amplitudes [2]. The model produces time series of a large number of signal features: amplitudes, phases, instantaneous power-delay profiles, Doppler spectra, etc. In [10] and [11] the propagation characteristics for land mobile satellite systems from L-Band to EHF-Band are given for narrow-band and wide-band applications in different scenarios and environments. A semi-Markov approach for single satellites which is currently part of ITU-R 681 has been introduced in [12]. There, the duration of times spent in each state follows the recommended probability distributions. In [13] and [14] in contrast to traditional multi-state Markov chain based models no prior assumptions are made on the number of states or on the statistical distributions characterizing each state. The sequence of single satellite channel states is blindly estimated using a Reversible Jump Monte Carlo Markov Chain algorithm. Although the model shows a good performance for a single satellite, its extension to multiple satellite systems would have a very high computational complexity. A comprehensive study on hidden Markov models is presented in [15]. In [16] the results of a study on time and spatial fade correlations of signals from two simultaneously transmitting satellites are presented.

Manuscript received September 26, 2008; revised July 14, 2009. First published October 16, 2009; current version published November 20, 2009. Parts of this paper have been published at the European Wireless Conference (EW2008), Prague, Czech Republic, June 2008, and at the International Workshop on Satellite and Space Communications, Toulouse, France, Oct. 2008.

M. Milojević and M. Haardt are with the Communications Research Laboratory, Ilmenau University of Technology, D-98684 Ilmenau, Germany (e-mail: marko.milojevic@tu-ilmenau.de; martin.haardt@tu-ilmenau.de).

A. Heuberger is with the Communications Research Laboratory, Ilmenau University of Technology, D-98684 Ilmenau, Germany. He is also with the Digital Broadcasting Research Laboratory, Ilmenau University of Technology, D-98684 Ilmenau, Germany (e-mail: albert.heuberger@tu-ilmenau.de).

E. Eberlein is with the Fraunhofer IIS, 91058 Erlangen, Germany (e-mail: ernst.eberlein@iis.fraunhofer.de).

Color versions of one or more of the figures in this paper are available online at http://ieeexplore.ieee.org.

Digital Object Identifier 10.1109/TBC.2009.2030464

An overview of the Satellite Digital Audio Radio Services (S-DARS) systems XM Radio and Sirius is given in [17] and [18].

In this paper we develop a satellite-to-outdoor channel model for systems with multiple satellites based on a Markov state model and Loo distributed channel amplitudes [2]. The simultaneous measurements of the S-DARS systems XM Radio and Sirius are studied to obtain all parameters of the proposed Markov model. In this paper we show that if the parameters of the Markov channel state model of order one or of a higher fixed order are used to create the channel state sequence, the corresponding PDF of the State Duration (PDFSD) in general does not coincide with the measured PDFSD. Therefore, we first approximate the PDFSD by a piecewise exponential function. Then we introduce a dynamic higher order Markov channel state model that is able to reproduce the original PDFSD. This model improvement is first studied for a single satellite system followed by the model extension for systems with multiple simultaneously transmitting satellites.

This paper is organized as follows: Section II introduces S-DARS channel measurements that are used for the parameter estimation throughout this paper. In Section III we describe our channel modeling concept for one and two satellite systems based on a first order Markov chain. Moreover, we study the S-DARS channel properties, namely the state duration, the correlation between satellite channels, and the spatial channel autocorrelation. In Section IV we show that the measured PDFSD cannot be reproduced well by a fixed order Markov model. Therefore we introduce the dynamic higher order Markov channel state model that shows a good modeling performance. We provide two algorithms for generating the channel state sequence with the same PDFSD as the original channel. Moreover, we discuss possible approximations of the models in order to reduce the number of required parameters for the channel state modeling. In Section V we extend the study to systems with multiple satellites. Finally, in Section VI we draw the conclusions. In the appendix we explicitly give the estimated parameters of our channel model for two simultaneously transmitting satellites based on the first order Markov chain obtained from the measured High Elliptical Orbit (HEO) and GEostationary Orbit (GEO) S-DARS systems for four different environments: urban, suburban with high buildings, suburban with low buildings, and a rural environment with trees. The parameters for dynamic order Markov chain are not given since they would take too much space.

II. S-DARS Channel Measurements

The channel parameters presented in the following have been validated by measurements of the S-DARS systems XM Radio (GEO system) and Sirius (HEO system) carried out on various locations in the USA and Canada for four different environments: urban, suburban with low buildings (up to 3 floors), suburban with high buildings (more than 3 floors), and a rural environment with trees. XM Radio and Sirius systems cover the continental USA and parts of Canada. The active observed HEO satellites have an elevation angle in the range between 28° and 75° (at least one satellite has an elevation over 64°), while the GEO satellites have elevations of 22° and 36° seen from Montreal, Canada. The HEO satellites are switched to the transmitting state for elevations higher than 25°.

The narrow-band measurements of XM Radio and Sirius systems have been carried out by Fraunhofer IIS, Germany, in August 2006 in the USA (Kokomo, Indiana, and California) and Canada (Ottawa, Montreal) by using a selective field strength meter (Rohde & Schwarz ESPI) with an equidistant trigger every 0.3846 m. Undersampling of the channel is justified as this does not affect the PDF of the measurement samples. The radio frequency signals from the satellites as well as from the terrestrial repeaters are received by a hybrid active antenna providing separate outputs for terrestrial and satellite signals. The center frequencies of the measured channel are in the range from 2320 MHz up to 2350 MHz, while the nominal filter bandwidth of each channel has been set to 500 kHz. In all measurements the signal power from four satellites (two GEO and two HEO satellites), from terrestrial repeaters, and the noise are simultaneously measured at every trigger instant (sample), while the GPS information is stored, allowing to decide very precisely to which environment the measurement data corresponds. The environment classification has been performed by visual inspection of the maps based on the obtained GPS information. In total, around 1 500 000 samples have been obtained.

III. Channel Model for Single and Two Satellite Systems Based on the First Order Markov Chains

The satellite-to-outdoor channel has been usually modeled with a Markov chain process and a statistical model. The Markov chain process describes the channel states and the transitions between the channel states while the statistical model describes the channel variations within each state. For a Markov chain of finite order m the following property holds for all n

$$\begin{aligned} P[S_n = s_n | S_{n-1} = s_{n-1}, S_{n-2} = s_{n-2}, \ldots, S_1 = s_1] \\ = P[S_n = s_n | S_{n-1} = s_{n-1}, \\ S_{n-2} = s_{n-2}, \ldots, S_{n-m} = s_{n-m}], \end{aligned} \tag{1}$$

where S_n is the state at time sample n, the values s_n form the state space of the chain, and $|$ denotes the conditional operator.

A. Channel State Model for Single Satellite Systems

The first order Markov chain process allows the signal to be in one of M defined states with a probability depending only on the previous state. This model has been widely accepted and used in the satellite communication community, e.g., [5]–[9]. Since the propagation conditions can in general be LOS, Non-Line-Of-Sight (NLOS), and in the transition area between the LOS and the NLOS, the channel state for one satellite is usually modeled by a Markov state channel model having three states: the Line-of-Sight (L), Blocked (B), and Shadowed (S) state. Solid obstacles such as houses, bridges, etc. will most probably cause total blockage of the signal, while trees typically lead to a shadowed state. The channel states depend on the

received signal power P_{rec}, and for a three state Markov model they are defined as:

$$\begin{aligned} &\mathrm{L}, \quad \text{if} \quad P_{\mathrm{rec}} \geq P_{\mathrm{LOS}} - P_1 \\ &\mathrm{S}, \quad \text{if} \quad P_{\mathrm{LOS}} - P_2 \leq P_{\mathrm{rec}} < P_{\mathrm{LOS}} - P_1 \\ &\mathrm{B}, \quad \text{if} \quad P_{\mathrm{rec}} < P_{\mathrm{LOS}} - P_2, \end{aligned} \tag{2}$$

where P_{LOS} is the mean signal power in the pure LOS environment in dBm, and P_1 and P_2 are the power thresholds defining the states, both in dB relative to P_{LOS}. These values influence the values of our model parameters and in the following we consider $P_1 = 3\,\mathrm{dB}$ and $P_2 = 10\,\mathrm{dB}$ since similar values have been used in the literature [5]–[9], [12].

The Markov channel state model of order one can be represented by a Stationary State Probability Vector (SSPV) $\boldsymbol{P}$ that contains the probabilities of the model being in a certain state and a State Probability Transition Matrix (SPTM) $\boldsymbol{P}_{\mathrm{trans}}$ that contains all probabilities of transition between the states. Assuming ergodicity, the SSPV is defined as:

$$\boldsymbol{P} = [P_B\ P_S\ P_L]^{\mathrm{T}}; \quad P_i = \lim_{N\to\infty} \frac{N_i}{N}, \qquad i \in \{\mathrm{L}, \mathrm{B}, \mathrm{S}\}, \tag{3}$$

where P_B, P_S, and P_L are the probabilities of the blocked, shadowed, and LOS state respectively, N_i is the number of measured channel samples being in state i, $\{\cdot\}^{\mathrm{T}}$ denotes the transpose operator, and N is the total number of samples. The measurements provide always a finite number of samples N. For a sufficiently large finite number of measured samples N, the probabilities P_i can be approximated as

$$P_i = \frac{N_i}{N}, \qquad i \in \{\mathrm{L}, \mathrm{B}, \mathrm{S}\}. \tag{4}$$

Similarly, for sufficiently large finite values N_i the SPTM can be approximated as

$$\boldsymbol{P}_{\mathrm{trans}} = \begin{bmatrix} p_{\mathrm{BB}} & p_{\mathrm{BS}} & p_{\mathrm{BL}} \\ p_{\mathrm{SB}} & p_{\mathrm{SS}} & p_{\mathrm{SL}} \\ p_{\mathrm{LB}} & p_{\mathrm{LS}} & p_{\mathrm{LL}} \end{bmatrix}; \qquad p_{ij} = \frac{N_{ij}}{N_i}, \tag{5}$$

where p_{ij} denotes the transition probability of a state changing from i to j, where $i, j \in \{\mathrm{L}, \mathrm{B}, \mathrm{S}\}$, N_{ij} is the number of transitions from state i to j, and N_i is the number of samples in state i. The SSPV and SPTM are obtained by post processing the channel measurements, and in general for different environments different $\boldsymbol{P}$ and $\boldsymbol{P}_{\mathrm{trans}}$ are obtained. Similarly as in equations (4) and (5), in equations (6), (7), (20), (26), and (27) the probabilities are estimated based on the approximations for large values of the denominators.

B. Channel State Model for the Two Satellite Systems

For the systems with two satellites, we want to capture the correlation between the states from the satellites. To this end, we introduce a Markov state channel model for two joint processes. This channel model has nine states, namely all possible permutations of the line of sight, blocked, and shadowed states for two satellites as shown in Fig. 1. The green, blue, and red color denote that the system consisting of two satellites is in the LOS, shadowed, and blocked state, respectively. For the sake of simplicity we consider that the channel state of the two satellite system is the best channel state of the two satellites. The stationary probabilities P_{ij} denote the probability that the channel states from the first and the second satellite at the same time are i and j, respectively, where $i, j \in \{\mathrm{L}, \mathrm{B}, \mathrm{S}\}$. The probabilities P_{ij} are estimated as

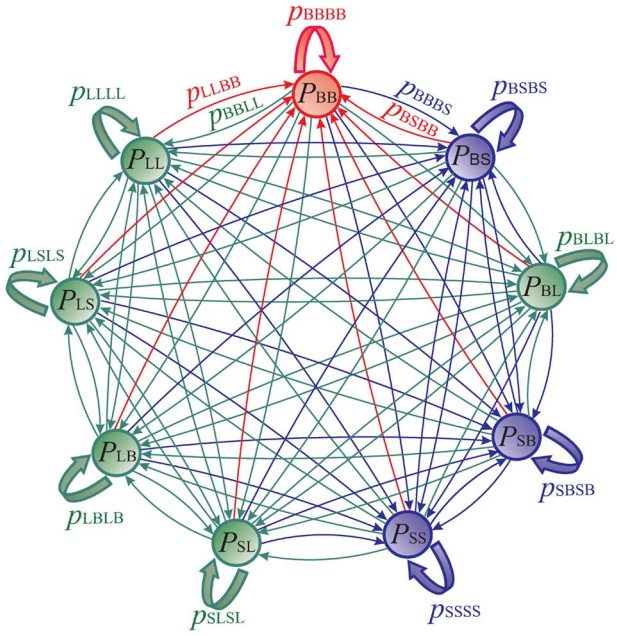

Fig. 1. Markov state channel model for two satellites.

$$P_{ij} = \frac{N_{ij}}{N}, \tag{6}$$

where N_{ij} is the number of measurement samples with channel states from the first and the second satellite being i and j respectively, and N is the total number of considered measurement samples. The transition probabilities $p_{i_1 j_1 i_2 j_2}$ between two consecutive time samples denote the probability of changing the state of the first satellite from i_1 to i_2 while simultaneously the state of the second satellite changes from j_1 to j_2. The values $p_{i_1 j_1 i_2 j_2}$ are estimated as

$$p_{i_1 j_1 i_2 j_2} = \frac{N_{i_1 j_1 i_2 j_2}}{N_{i_1 j_1}}, \tag{7}$$

where $N_{i_1 j_1 i_2 j_2}$ is the number of transitions from state $i_1 j_1$ to $i_2 j_2$ and $N_{i_1 j_1}$ is the number of samples in state $i_1 j_1$. The channel state model for multiple satellites introduced in Section V is based on this approach. Based on measurements, we estimate the parameters of the joint Markov state channel model for two satellite constellations in GEO and HEO in four environments: urban, suburban with high buildings, suburban with low buildings, and a rural environment with trees. Both the GEO and the HEO constellations have two simultaneously transmitting satellites.

The joint state probability matrix is defined as

$$\boldsymbol{P} = \begin{bmatrix} P_{\mathrm{BB}} & P_{\mathrm{BS}} & P_{\mathrm{BL}} \\ P_{\mathrm{SB}} & P_{\mathrm{SS}} & P_{\mathrm{SL}} \\ P_{\mathrm{LB}} & P_{\mathrm{LS}} & P_{\mathrm{LL}} \end{bmatrix}, \tag{8}$$

and the joint state transition probability matrix is equal to

$$\boldsymbol{P}_{\text{trans}} = \begin{bmatrix} p_{11} & p_{12} & p_{13} & p_{14} & p_{15} & p_{16} & p_{17} & p_{18} & p_{19} \\ p_{21} & p_{22} & p_{23} & p_{24} & p_{25} & p_{26} & p_{27} & p_{28} & p_{29} \\ p_{31} & p_{32} & p_{33} & p_{34} & p_{35} & p_{36} & p_{37} & p_{38} & p_{39} \\ p_{41} & p_{42} & p_{43} & p_{44} & p_{45} & p_{46} & p_{47} & p_{48} & p_{49} \\ p_{51} & p_{52} & p_{53} & p_{54} & p_{55} & p_{56} & p_{57} & p_{58} & p_{59} \\ p_{61} & p_{62} & p_{63} & p_{64} & p_{65} & p_{66} & p_{67} & p_{68} & p_{69} \\ p_{71} & p_{72} & p_{73} & p_{74} & p_{75} & p_{76} & p_{77} & p_{78} & p_{79} \\ p_{81} & p_{82} & p_{83} & p_{84} & p_{85} & p_{86} & p_{87} & p_{88} & p_{89} \\ p_{91} & p_{92} & p_{93} & p_{94} & p_{95} & p_{96} & p_{97} & p_{98} & p_{99} \end{bmatrix}, \tag{9}$$

where the states 1 to 9 are: $1 = \text{BB}$, $2 = \text{BS}$, $3 = \text{BL}$, $4 = \text{SB}$, $5 = \text{SS}$, $6 = \text{SL}$, $7 = \text{LB}$, $8 = \text{LS}$, and $9 = \text{LL}$. They are estimated for all four environments. The first subscript digit of the transition probability matrix elements denotes the states of satellites 1 and 2 at one time instance, and the second subscript digit denotes the states of satellites 1 and 2 in the following time instance. The numerical estimation results for measured S-DARS systems are provided in the appendix. The matrices $\boldsymbol{P}$ and $\boldsymbol{P}_{\text{trans}}$ are estimated in the following fashion:

- For each measured sample, we determine the channel state based on its power level and equation (2). After determining the states of all samples, we obtain the state probability matrix $\boldsymbol{P}$ by applying equation (6).
- For each sample, we test whether the measured power level crosses the threshold between different states. If the channel state changes from state $i_1 j_1$ to $i_2 j_2$ we increase the counter for that transition by 1 and remember for how long the state remained the same. The transition probabilities are estimated using equation (7).

The analysis results of the measurements, which are given in the appendix, show that the channel from HEO satellites is less blocked than the channel from geostationary satellites while the opposite holds for the probability of the LOS state. This is due to the higher elevation of the HEO satellites over the covered areas which lowers the blockage probability of the LOS signal component. The measurement results also show that the urban environment has the highest probability of blockage while the suburban environment with low buildings has the lowest probability of blockage, which is conditioned on the receiver's surrounding environment. In all environments many transition probability elements of the measured S-DARS systems are close to zero, which can be seen in the results presented in the appendix.

C. The Channel Amplitude Modeling

The time evolution between consecutive samples of the channel within one state (fast fading) is not the priority in our study since broadcasting systems with interleavers longer than 2 s are considered. The channel statistics, e.g., the PDF of the channel fading amplitude, provide the required information on the channel variations within one state. The amplitude PDF in satellite-to-outdoor communications for each state is characterized by various combinations of Ricean, Rayleigh, and log-normal PDFs [19]. The difference between the models lies in the interpretation of the shadowing mechanism on direct and scattered paths. These statistical descriptions are valid under certain assumptions, for example, that the central limit theorem holds. In this contribution, the signal variations due to shadowing and multi-path effects within each individual Markov state are assumed to follow a Loo [2] distribution with different parameters for each Markov state. All samples of a given channel state are used for the statistical modeling of that particular state: the PDF of the channel magnitudes is fitted to the Loo distribution by estimating the parameters μ, d_0, and b_0 which are defined in the following. Loo's model considers the resulting signal as a sum of Rayleigh and Log-normal distributed phasors:

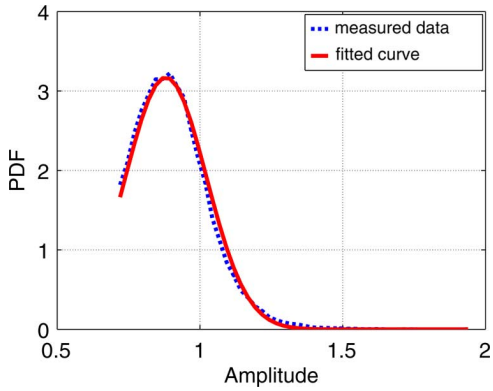

Fig. 2. Amplitude PDF fitting for the LOS state for one geostationary satellite in the urban environment.

$$r^{j\theta} = z^{j\phi_0} + w^{j\phi}, \qquad z > 0, w > 0, \tag{10}$$

where the phases ϕ_0 and ϕ are uniformly distributed between 0 and 2π, z is log-normally distributed, and w has a Rayleigh distribution. The log-normal distribution of z is defined as:

$$f(z) = \frac{1}{\sqrt{2\pi d_0} z} e^{-\frac{(\ln z - \mu)^2}{2d_0}}, \tag{11}$$

where $\sqrt{d_0}$ and μ are the standard deviation and mean, respectively. If z is temporarily kept constant, then the conditional PDF of r is Rician:

$$f(r|z) = \frac{r}{b_0} e^{-\frac{r^2+z^2}{2b_0}} I_0\left(\frac{rz}{b_0}\right), \tag{12}$$

where b_0 represents the average scattered power due to multipath, and $I_0(\cdot)$ is the modified Bessel function of the zeroth order. After integration over z and the substitution of $f(z)$ the PDF of the received signal r is

$$f(r) = \frac{r}{b_0\sqrt{2\pi d_0}} \int_{z=0}^{\infty} \frac{1}{z} e^{-\frac{(\ln z - \mu)^2}{2d_0} - \frac{r^2+z^2}{2b_0}} I_0\left(\frac{rz}{b_0}\right) dz. \tag{13}$$

The parameters μ, d_0 and b_0 define Loo's PDF (13). In Fig. 2 we show the amplitude PDF fitting with the Loo distribution for the LOS state of one geostationary satellite in the urban environment. The measurement values $20\log_{10}(e^{\mu})$, $20\log_{10}(e^{\sqrt{d_0}})$, and $10\log_{10}(2b_0)$ of HEO and GEO S-DARS systems for different environments are provided in the appendix. All HEO measurements of a given environment are used to extract the parameters for that environment, in spite of the fact that the

HEO satellites elevation is time variant. The extraction of the parameters as a function of the elevation would be more accurate. A prerequisite is, however, that a sufficient amount of data is available. If an infinite number of measurements is taken, the averaged parameters of the HEO 1 and HEO 2 satellites tend to converge to the same values.

We intentionally study two data sets corresponding to two HEO satellites independently to show that their parameters differ in general for a given environment. For the two satellite systems the channel states are correlated as introduced in Section III-B while the amplitudes within the states are generated independently. This is a good approximation since we assume interleavers longer than 2 s. Additionally, in the following section we study the correlation properties of the channels from different satellites. The estimated correlation coefficients can be used for creating, for example, a 2-D Loo's amplitude distribution with corresponding correlation properties.

D. Correlation and State Duration Properties of the S-DARS Channels

In this section we study the correlation between S-DARS satellite channels, the spatial channel autocorrelation, and the channel state duration.

1) Correlation Coefficient Between Two S-DARS Satellites: The correlation between the fading channel coefficients from different satellites has a strong bearing on the achievable diversity gain. We have measured only the magnitude of the signals and therefore the correlation coefficient ρ between the received signals from two satellites of the same constellation (one set are two geostationary XM Radio satellites while another set are two HEO Sirius satellites) can be estimated with the following formula

$$\rho = \frac{\mathrm{E}[r_1 r_2] - \mathrm{E}[r_1]\mathrm{E}[r_2]}{\sqrt{\left(\mathrm{E}\left[r_1^2\right] - \mathrm{E}[r_1]^2\right)\left(\mathrm{E}\left[r_2^2\right] - \mathrm{E}[r_2]^2\right)}}, \tag{14}$$

where r_1 and r_2 are the magnitudes of the measured channels from two satellites of the same system, and $\mathrm{E}[\cdot]$ is the expectation operator. The correlation factors are estimated over measurement segments of 30 wavelengths that are not overlapping. The PDF of the correlation $f(\rho)$ can be well approximated by a fourth order polynomial in all environments:

$$f(\rho) \approx p_1\rho^4 + p_2\rho^3 + p_3\rho^2 + p_4\rho + p_5. \tag{15}$$

The coefficients of the polynomial for the geostationary and HEO satellite system are given in Tables I and II, respectively, for all four studied environments. As an example, Fig. 3 depicts the fourth order polynomial approximation of the estimated PDF of the correlation factor between two Sirius HEO satellites and between two geostationary (GEO) XM Radio satellites in the urban environment. By observing the PDFs for different environments, it can be noticed that they all have very similar shapes. The PDF of the correlation coefficients between the geostationary satellites has been shifted to the right when compared to the corresponding curve for the HEO satellites, meaning that the channels from the geostationary satellites are more correlated. This is a consequence of a lower elevation angle characteristic for geostationary satellites, which results in a higher influence of the surrounding environment at the receiver.

TABLE I
POLYNOMIAL COEFFICIENTS FOR GEOSTATIONARY SATELLITES

	p_1	p_2	p_3	p_4	p_5
Urban	0.003	-0.364	-0.666	0.445	0.721
Sub. Low	0.143	-0.213	-0.953	0.21	0.79
Sub. High	0.34	-0.175	-1.203	0.156	0.834
Rural	0.353	-0.122	-1.20	0.116	0.83

TABLE II
POLYNOMIAL COEFFICIENTS FOR HEO SATELLITES

	p_1	p_2	p_3	p_4	p_5
Urban	0.454	-0.058	-1.298	0.053	0.842
Sub. Low	0.445	0.03	-1.306	-0.021	0.847
Sub. High	0.342	-0.009	-1.199	0.014	0.832
Rural	0.57	0.018	-1.426	-0.003	0.861

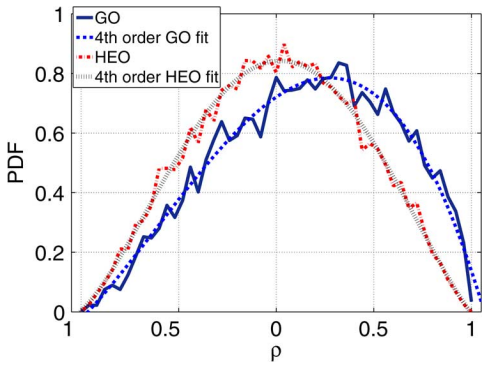

Fig. 3. PDF of the correlation factor between two Sirius HEO/two XM Radio GEO satellites in the urban environment and their fourth order polynomial fit.

TABLE III
VALUES $d_{0.5}$ IN METERS FOR STUDIED SATELLITES AND ENVIRONMENTS

	Urban	Sub. High	Sub. Low	Rural
GEO 1	15	4.61	0.38	4.61
GEO 2	21.15	10.77	2.69	7.31
HEO 1	10.77	1.15	0.38	1.54
HEO 2	8.08	3.85	0.38	0.38

2) Spatial Autocorrelation Function of S-DARS Satellites: In order to determine the size of the required interleaver at the receiver we study the spatial autocorrelation function. Of special importance is the distance $d_{0.5}$, for which the spatial autocorrelation drops to the value 0.5: it gives an indication of the interleaver length required to overcome the channel memory effect. The spatial autocorrelation function is estimated for all measurement runs within one environment. The obtained distances $d_{0.5}$ for the measured S-DARS channels are higher for geostationary satellites and their values are between 0.38 and 22 meters. Table III summarizes the mean values of $d_{0.5}$ (in meters) for channels from both geostationary (GEO 1 and GEO 2) and HEO (HEO 1, HEO 2) satellites in all four studied environments.

3) Channel State Duration of the S-DARS Systems: The average state duration can be estimated with the use of the matrices $\boldsymbol{P}$ and $\boldsymbol{P}_{\mathrm{trans}}$, similar as in [6]. We show in Section IV

that the fixed order Markov chain model is not capable to model well the state durations. Since the PDF of the state duration (especially for the blocked state) is an important parameter in the system planning step, we analyze the measurements to obtain the PDF of the state duration and approximate it with a piecewise exponential function. By using this approximation one can produce the channel state sequence (with an algorithm introduced in Section IV) for S-DARS systems that is more appropriate than the one that would be obtained based on parameters of a first order Markov chain.

We make no assumptions on the minimum state duration in order to avoid occurrences where short intervals of very deep or medium fades are characterized with LOS states and vice versa, as in, e.g., [7]–[9]. The measurement results show that the LOS state duration of HEO satellites is longer than of the GEO satellites due to the higher elevations of the HEO satellites. The opposite holds for the blocked state duration. The longest blockage duration of 110 m is measured for each of the GEO satellites in an urban environment while the longest measured blockage of the system consisting of both satellites together is 70 m which is a significant reduction. In both cases, such blockages require long interleavers to enable reception. In other environments, the longest measured blockage duration of GEO system is 10 m, while for the HEO system, the longest measured blockage duration is 13 m. The longest measured LOS state duration is 8200 m for the HEO satellite in the suburban environment with low buildings. LOS state durations of a few kilometers are relatively often observed in rural and suburban environments.

The PDFs of the state duration for all environments can be approximated by a piecewise exponential function with four segments

$$L(d) = \begin{cases} L_1 e^{-db_1}, & d_{\min} \le d \le d_1 \\ L_2 e^{-db_2}, & d_1 < d \le d_2 \\ L_3 e^{-db_3}, & d_2 < d \le d_3 \\ L_4 e^{-db_4}, & d_3 < d \le d_4, \end{cases} \tag{16}$$

where $L(d)$ denotes the probability of the state duration d, L_1, L_2, L_3, and L_4 are the marginal probabilities if the state duration was zero, b_1, b_2, b_3, and b_4 are the decaying factors of different function segments defined with state durations d_1, d_2, d_3, and d_4 expressed in meters, and $d_{\min} = 0.3846$ m corresponds to the minimum measured state duration. Four segments show a good tradeoff between the accuracy and the number of parameters needed to describe the function. For a more precise approximation, a higher number of segments should be used. Properly chosen values of $L_1, \ldots, L_4$, $b_1, \ldots, b_4$, and $d_{\min}$, $d_1, \ldots, d_4$ ensure the continuity of the function $L(d)$. In Fig. 4 we show such a fit by using a four segment piecewise exponential function. The fit can follow only the slow change of the measured PDF since the exponential functions on the logarithmic scale are straight lines. In Table IV we state the approximation parameters for the urban environment for all analyzed satellite signals: GEO 1, GEO 2, and GEO denote the receivers for only the first, only the second, and both geostationary satellites, respectively. GEO assumes satellite selection- the best channel state from two satellites is the state of the whole system. When comparing the

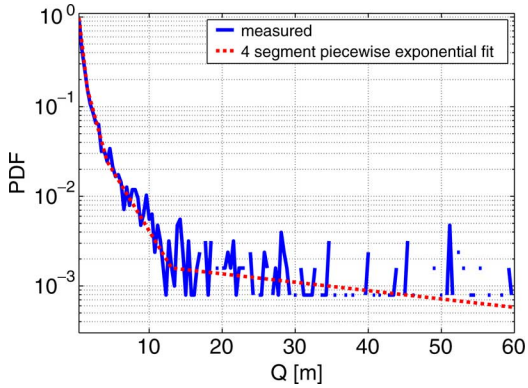

Fig. 4. Piecewise exponential fit of the PDF of the blocked state.

TABLE IV
STATE DURATION APPROXIMATION PARAMETERS FROM EQUATION (16) FOR THE GEOSTATIONARY SYSTEM IN URBAN ENVIRONMENT

	Blocked			Shadowed			LOS		
	GEO 1	GEO 2	GEO	GEO 1	GEO 2	GEO	GEO 1	GEO 2	GEO
$L_1 \cdot 10^3$	1496	1960	2432	4350	3174	4254	1176	1473	1088
$L_2 \cdot 10^3$	379	516	373	1043	773	1627	200	245	419
$L_3 \cdot 10^3$	92.6	114	253	138	227	668	23.9	33	30
$L_4 \cdot 10^3$	4.7	2.97	2.33	2.76	5.4	38	0.89	1.22	0.77
$b_1 \cdot 10^3$	1581	1945	1907	2644	2380	2931	1284	1411	1143
$b_2 \cdot 10^3$	689	788	689	1406	1155	1682	364	479	648
$b_3 \cdot 10^3$	356	395	597	748	625	1103	113	153	120
$b_4 \cdot 10^3$	17.8	16.1	43	150	52.5	357	13.2	21.3	10.7
d_1	1.6	1.3	1.6	1.3	1.2	0.8	2	2	2
d_2	4.3	4	4.3	3	2.4	1.6	8.5	6.2	5.1
d_3	9	9.5	8.5	6.6	6.7	4	33	25.1	33.5
d_4	110	110	70	55	55	50	200	200	300

PDFs of the state duration for the GEO, GEO 1, and GEO 2 schemes the following can be observed:

- For the blocked state, the PDF of the GEO scheme has higher values for small state durations and lower values for longer state durations. In the GEO scheme with two simultaneously transmitting satellites, the probability that one satellite is not blocked is higher than in a single satellite system.
- For the shadowed state, all PDFs are very similar.
- In the LOS state, the GEO scheme has slightly higher PDF values than the GEO 1 and the GEO 2 scheme for higher state durations due to the diversity.
- The PDF decays the fastest for the shadowed state in urban environments.

IV. THE STATE DURATION OF THE MARKOV CHAIN BASED CHANNEL MODELS

Thanks to time interleaving in satellite systems only the long time periods of blockage will result in non-availability. Therefore, it is of high importance that the occurrences of long blockages are well represented by the channel model, i.e., the PDF of the generated channel blockage duration should be as close as possible to the original PDF of the blockage duration obtained from the measured channels. In the process of system planning channel state sequences generated by the channel model are used. Without loss of generality, in the following we concentrate on the urban environment, as it represents the worst case

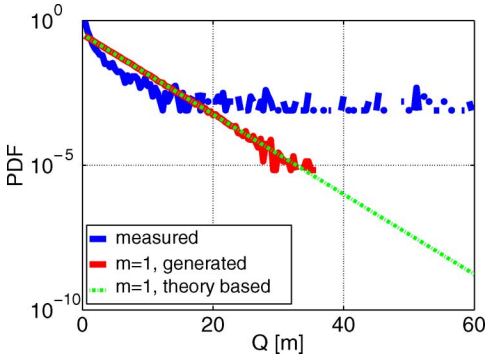

Fig. 5. The PDF of the blocked state duration for one GEO satellite and urban environment based on measurements, theory, and simulation.

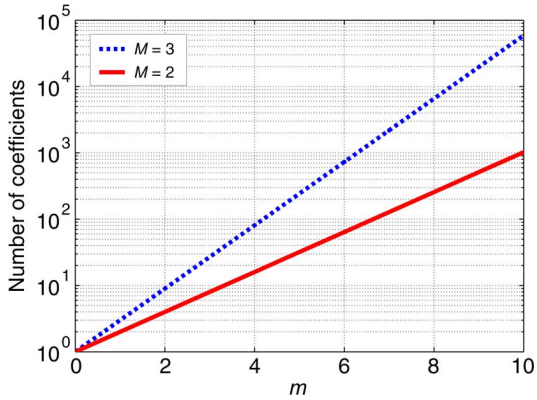

Fig. 6. The number of transition coefficients needed to fully describe the Markov state model of order m.

with respect to long blockages. First we will study the modeling performance of the state channel models based on the fixed order Markov chains. In the following, we compare the statistics of channel state sequences obtained by different channel state modeling algorithms with the statistics of measured channels. This comparison will indicate the accuracy of studied modeling approaches.

For a Markov channel state model of order one, the probability p_i that the model stays in state i for exactly q consecutive samples can be written as

$$p_i(Q = q\Delta d) = p_{ii}^{q-1} \cdot (1 - p_{ii}), \tag{17}$$

where Q denotes the state duration and Δd the sampling interval. In Fig. 5 we show the PDF of the blockage durations for one GEO satellite corresponding to the urban environment:

- The solid blue line represents the PDF of the measured channels.
- The green dash-doted line represents the Markov order one theory based PDF calculated with (17).
- The solid red line shows the PDF of a generated state sequence based on the use of the SPTM of a Markov channel state model of order one. The generated state sequence has 10 000 000 samples. This value is used for all generated channel state sequences in the following.

Generally, a Markov channel state model of order $m = 1$ is able to match the stationary state probability vector and the mean state duration. However, as shown in Fig. 5, it does not reproduce long blockages that occur in the measurements.

For a higher order Markov model $(m > 1)$ the SPTM can be estimated similarly as for the order $m = 1$ case. In general, for a one satellite system the SPTM of a full order m Markov model has M^{m+1} transition coefficients. Due to the exponential function, the number of coefficients increases very fast for increasing order and only a low order Markov model (order up to a maximum of 10) can be considered. The number of transition coefficients can be reduced if only two states are considered $(M = 2)$, but even in that case the number of transition coefficients is very large for $m > 15$. In Fig. 6 we show the number of SPTM coefficients for the full m-th order Markov chain for $M = 2$ and $M = 3$ as a function of the order m.

In Fig. 7 we compare the PDFs of the blockage durations for one GEO satellite corresponding to the urban environment.

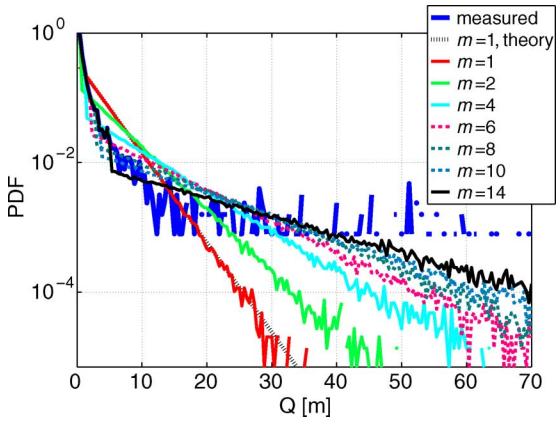

Fig. 7. The PDF of the blocked state duration for different order m Markov channel state models for one GEO satellite and urban environment.

The PDFs are generated via simulations for different Markov models of order m having three states. The corresponding parameters are obtained from measurements. The following can be concluded:

- For $m = 1$ the theory based PDF calculated with (17) matches well the blockage PDF of the generated sequence for $m = 1$ as expected, but both do not match well enough the PDF of the measured blockage duration.
- None of the order m Markov models up to $m = 14$ is able to generate the correct blockage PDF. The generated PDFs are correct up to a duration of $m-1$ samples, and therefore the curves for higher m fit better for low values of Q.
- At higher state durations, which are of the highest interest all models with $m < 14$ are far away from correctly generating the measured PDFSD.
- For an exact representation of the PDFSD the order $m = q_{max}$ should be used, where q_{max} denotes the maximum state duration in samples. For our urban measurements $q_{max} = 284$. For the corresponding order 284 Markov model 3^{285} coefficients would be needed which is not a realistic option due to the high computational complexity. As already mentioned, Markov model based state models are not practical for orders higher than 10.

Similar conclusions can be drawn also for the PDF of the shadowed or the LOS state duration. Due to the complexity

constraint, in general we can conclude that the classical Markov model cannot generate the PDFSD that matches the measured PDFSD. The major problem of the fixed order Markov channel state model is its incapability of modeling long blockages that occur in the measurements. A high percentage of samples with blocked state correspond to long blockages, despite the fact that long blockages occur relatively rare. In our measurements 48.5% of the samples with blocked states correspond to blockage durations longer than 20 m, since, e.g., 100 successive blockage samples correspond to a single blockage duration of 38.5 m. The Markov state model of any fixed order is able to match only the stationary state probability vector.

In [5]–[9] the mismatch of the PDFSDs comes from the simplified assumption that the appropriate Markov channel state model is of order one. This assumption is made in order to have a simple model with a low number of states. The measurement based PDF of the blockage shows higher probabilities for low blockage durations in Fig. 5, lower probabilities for medium blockage durations, and again higher probabilities for high blockage durations when compared to the theory-based probabilities using the Markov state model of order one. This implies the conclusion that the state transition probability matrix is not fixed. The physical interpretation of this behavior is the following: the clustered nature of ground objects in urban environments determines the channel states and such a structure cannot be completely described by a Markov state chain of order one. For example, some large objects or sets of objects lead to very long blockages on the order of 100 meters, which we cannot obtain in the simulations by using a Markov state machine of order one. As just concluded, also the fixed higher order Markov model does not solve this problem. Therefore, in order to improve the PDFSD match we introduce a Markov channel state model with a dynamic SPTM.

A. *The PDFSD Modeling Based on Dynamic Order Markov Chains*

The Markov channel state model with a dynamic order that we consider has the SPTM $\boldsymbol{P}_{\text{trans}}$ as a function of the current state duration Q

$$\boldsymbol{P}_{\text{trans}} = F(Q), \tag{18}$$

where F denotes the corresponding function and we describe it with the state probability transition tensor (SPTT)

$$\boldsymbol{\mathcal{P}}_{\text{trans}}(:,:,q) = \boldsymbol{P}_{\text{trans}}(q\Delta d), \qquad q = 1, 2, \ldots, q_{max}, \tag{19}$$

where q_{max} is the maximum value of q ($Q = q\Delta d$), $\boldsymbol{\mathcal{P}}_{\text{trans}} \in \mathbb{R}_{+}^{M\times M\times q_{max}}$, and M is the number of channel states. The current state duration (distance) of state i at any observed position d equals Q if the channel has entered state i at $d-Q$ and did not change within the interval $[d-Q, d]$. The tensor $\boldsymbol{\mathcal{P}}_{\text{trans}}$ contains the stacked SPTMs $\boldsymbol{P}_{\text{trans}}(Q)$ calculated for different values of the current state duration Q and its elements are real and non-negative. They can be estimated from the measurement data and are in general different for different environments. The structure of a state probability transition tensor $\boldsymbol{\mathcal{P}}_{\text{trans}}$ is depicted in Fig. 8. The algorithm to obtain the dynamic SPTM elements is almost the same algorithm as for the Markov state model of order one with an additional step where the current state duration has to be taken into account. For the one satellite system, the dynamic transition probability elements $p_{ij}(Q)$ are estimated as

$$p_{ij}(Q = q\Delta d) = \frac{N_{ij}(Q)}{N_i(Q)}, \qquad i, j \in \{\text{L}, \text{B}, \text{S}\}, \tag{20}$$

where $N_{ij}(Q)$ is the number of transitions from state i to j after q consecutive channel samples in state i, and $N_i(Q)$ is the number of channel samples in state i given the constraint that the current state i duration is Q. The algorithm for creating the channel state sequence based on the state probability transition tensor can be described in three steps:

1) Assume that the channel enters state i at time t_0 (therefore the current state duration is equal to 0),
2) Estimate the channel state at the next time sample by using the state probability transition matrix $\boldsymbol{P}_{\text{trans}}(Q)$ given the current state duration Q,
3) Repeat the procedure starting from step 2).

Using this algorithm, the probability $p_i(Q = q\Delta d)$ that the model stays in state i for exactly q consecutive samples can now be written as

$$p_i(q\Delta d) = (1 - p_{ii}(q\Delta d)) \cdot \prod_{r=1}^{q-1} p_{ii}(r\Delta d), \tag{21}$$

while the corresponding Cumulative Distribution Function (CDF) of the state duration for each state i is

$$C_i(q\Delta d \le q_0\Delta d) = \sum_{k=1}^{q_0} (1 - p_{ii}(k\Delta d)) \cdot \prod_{r=1}^{q-1} p_{ii}(r\Delta d). \tag{22}$$

The resulting PDF of the blockage duration of the generated channel state sequence with the SPTT based algorithm which is denoted by a dashed light blue line in Fig. 9 matches perfectly the resulting PDF of the blockage duration estimated with (21) and the measured PDF of the blockage duration. Furthermore,

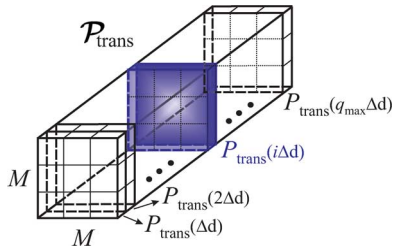

Fig. 8. The structure of the state probability transition tensor $\boldsymbol{\mathcal{P}}_{\text{trans}}$.

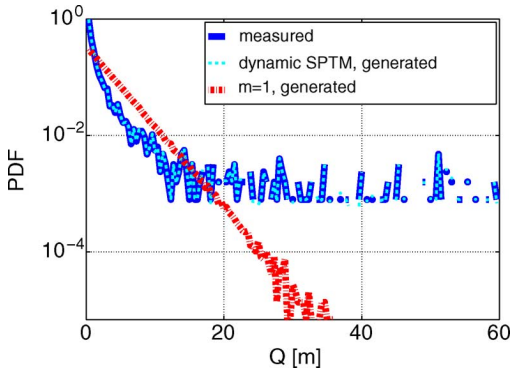

Fig. 9. The PDF of the blocked state duration for one GEO satellite and urban environment.

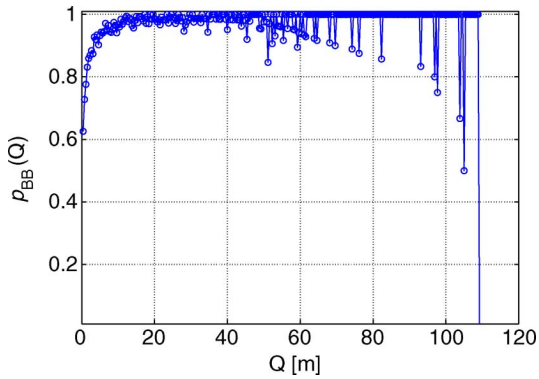

Fig. 10. State transition coefficient p_{BB} as a function of the current blockage duration [m] for the GEO satellite and urban environment.

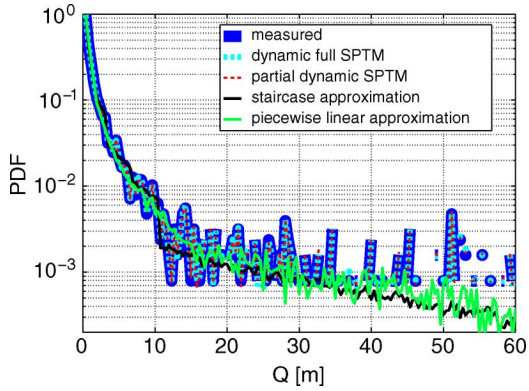

Fig. 11. The PDF of the blocked state duration of measurements and dynamic SPTM models.

the match is also perfect for the PDFSD of the shadowed and the LOS state. Additionally, the stationary measurement based probability vector is matched perfectly as well if this algorithm is used. Therefore, we can conclude that the presented dynamic order Markov state model can cope well with the state duration modeling problem.

Although we deal with a fixed set of SPTMs represented by the SPTT of dimension $M \times M \times q_{max}$, the order of this model is dynamic. This is due to the assumption that the state memory is reset (the chain order is set to one) after each state change along the displacement vector. This is crucial for the practicability of the algorithm, as we reduce the number of full order m Markov model transition coefficients which equals to M^{m+1}. In Fig. 10 we show the probability p_{BB} of staying in the blocked state as a function of the current blockage duration. At a distance of 110 m it drops to zero since this is the longest measured blockage. Similar figures can be obtained for the other transition probabilities defined in (20). All values of the transition coefficients $p_{ij}(Q)$ can be written in vector form:

$$\boldsymbol{p}_{ij} = [p_{ij}(\Delta d) p_{ij}(2\Delta d) \ldots p_{ij}(q_{max}\Delta d)]^{\mathrm{T}}. \tag{23}$$

B. Dynamic SPTM Model Approximations

In this section we will introduce approximations of the dynamic SPTM model: they model well the PDFSD but have reduced number of coefficients.

1) Partial Dynamic SPTM Model: Equation (21) suggests that only the transition probabilities of remaining in the same state, namely p_{BB}, p_{SS} and p_{LL}, are needed as a function of the current state duration to estimate the PDFSD. In addition, measurement results suggest that the values p_{BS} and p_{LB} are very close to zero, and that the values p_{SB} are rather small. Therefore, in order to reduce the number of parameters of the dynamic SPTM model the following approximations can be introduced:

- Only the transition coefficients $p_{XX}(Q)$, $X \in \{B, S, L\}$ change as the function of the current state duration, and therefore have to be estimated for all values of Q.
- The coefficients p_{XY}, $X \neq Y$ can either be fixed or they can be changed together with the coefficients $p_{XX}(Q)$ by keeping the respective relative ratio S_L between them constant. They have to be estimated only once for $Q = \Delta d$. In the latter approach, the coefficients $p_{XY}(\Delta d)$ are used to obtain the relative ratios S_L which are then used for all $Q = q\Delta d$, $q = 2, 3 \ldots q_{max}$. For that approach, the transition coefficients for the blocked state are estimated as:

$$\begin{aligned} S_L &= \frac{p_{BS}(\Delta d)}{p_{BL}(\Delta d)}, \\ p_{BL}(Q) &= \frac{1 - p_{BB}(Q)}{1 + S_L}, \\ p_{BS}(Q) &= S_L \cdot p_{BL}(Q). \end{aligned} \tag{24}$$

Similar sets of equations with different subscript indices are valid for the shadowed and the LOS state.

Assuming these approximations and probability vectors $\boldsymbol{p}_{BB}$, $\boldsymbol{p}_{SS}$, and $\boldsymbol{p}_{LL}$ that are estimated from the measurements, we obtain a PDFSD that matches well the measured PDFSD. The PDF of the blockage after using this method is shown in Fig. 11 (denoted with "partial dynamic SPTM") and it overlaps the measured PDF of the blockage duration. A perfect PDFSD match is achieved also for the shadowed and the LOS state duration. As a consequence, the mean state durations also coincide. Therefore, we can conclude that the partial dynamic SPTM model allows to reconstruct the PDF of the state duration very precisely. For our measurement data, it has approximately as many coefficients as a fixed order $m = 5$ full Markov model but it models the PDFSD much better. The full dynamic SPTM model based channel has more information about the channel, which is responsible for the long term channel behavior. It contains the information of the exact transition probabilities obtained from the measurements while the partial dynamic SPTM state model contains some exact and some approximated coefficients. Nevertheless, the partial dynamic SPTM state model is able to match perfectly the PDF of the state duration and the mean state duration.

2) Approximated Partial Dynamic SPTM Model: Now we study how the amount of information necessary to represent the proposed partial dynamic SPTM model can be reduced further, while still keeping a good match between the simulated and the measured PDFs of the state durations. The partial dynamic SPTM model has as input parameters vectors $\boldsymbol{p}_{XX}(Q)$, $X \in \{B, S, L\}$. As an example, the maximum blockage duration of the GEO 1 satellite in our measured data in the urban scenario is 109.2 m which corresponds to 284 samples (samples are equidistant with a distance difference between consecutive samples of 0.3846 m). This means that the vector $\boldsymbol{p}_{BB}$ should

have 284 values to allow the exact reproduction of the measured PDF of the blockage. The idea is to approximate $\boldsymbol{p}_{XX}(Q)$, $X \in \{B, S, L\}$ by only a few coefficients. We consider two approaches:

1) Staircase approximation: we pick a small subset of l values $p_{XX}(k\Delta d)$, where $k \in K = \{k_1, k_2, \ldots, k_l\} \subset \{1, 2, \ldots, q_{max}\}$, and $X \in \{B, S, L\}$, that are possibly different for each state X. The values $p_{XX}(q\Delta d)$, $k_r \leq q \leq k_{r+1}$ between the chosen subset points k_r and k_{r+1} are set to the fixed value $p_{XX}(k_r\Delta d)$. The approximated vector $\boldsymbol{p}_{BB}$ obtained by using this method is compared in Fig. 12 with the complete description of the vector $\boldsymbol{p}_{BB}$ according to Section IV-A. One set of positions K that provides a good fit for our measurements is $(1, 2, 3, 4, 5, 9, 18, 28, 43) \cdot 0.3846$ m. As a rule of thumb, the values should be picked denser for low state durations since in this region they show the biggest change. The resulting PDF obtained by the channel state sequence generation based on this method is depicted in Fig. 11 and denoted with "staircase approximation". The PDFs do not exactly match the measured PDFs of the blockage duration: the generated PDFs match rather the slow change of the measured PDFs. Despite the low computational complexity of this approach and the small set of parameters, the result is still better than any of the results based on the fixed higher order m Markov model from Fig. 7.
2) Piecewise linear approximation: the staircase approximation can be improved if the intervals between the chosen subset points $p_{XX}(k)$, $k \in K \subset \{1, 2, \ldots, q_{max}\}$ are approximated by piecewise linear functions as shown in Fig. 12. For the piecewise linear approximation of $\boldsymbol{p}_{BB}$ we used only 8 points at state durations $(1, 5, 10, 16, 33, 50, 98, 155) \cdot 0.3846$ m. As shown in Fig. 11 the generated PDF matches quite well the measured one. It is able to reproduce to some extent also the long blockages. The match cannot follow the fast changes of the PDF; it follows only the slow change in the PDF. The sum of the PDFs of the measured and the generated sequences for all current state durations longer than 20 m has almost the same value. When an extremely high number of the measured samples is analyzed, the PDF has a smoother shape. In that case, the linear piecewise fit or some other simple fit would perform even better leading to a better match of the generated PDFSD. One can argue that the transition vectors $\boldsymbol{p}_{XX}$ obtained with this approach still have the same number of elements as the full transition vectors since the elements between the chosen points have to be estimated by interpolation. The advantage lies in the fact that only a few coefficients are enough to approximate the missing ones and therefore it is beneficial for channel modeling.

Since a good model of the blockage state duration is of the highest priority we could consider that only the blockage transition coefficients p_{BB} are dynamic. Such a model will not be able to precisely model the PDF of the shadowed and the LOS state duration, but due to the very small number of coefficients it can be considered as an alternative solution.

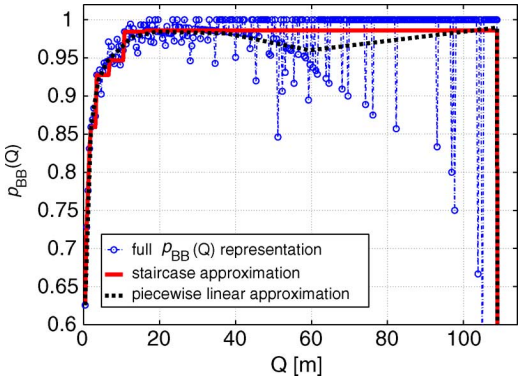

Fig. 12. Transition coefficient p_{BB} and its approximations as a function of the current blockage duration.

In the following we will extend the dynamic SPTM approach to satellite systems with multiple simultaneously transmitting satellites. Before we come to that point we describe the PDFSD based state channel generation algorithm which has a low computational complexity (lower than the computational complexity of algorithms based on the dynamic SPTM $\boldsymbol{P}_{\text{trans}}(Q)$ just described) and provides a perfect match of the PDFSD (overlaps the dashed light blue curve in Fig. 5). If extended to systems with multiple satellites, the relative difference in computational complexity between two approaches disappears. The advantage of the dynamic SPTM based model is that it gives better insight in the modeling problem.

C. PDFSD Based Channel State Generation Algorithm

The algorithm needs as input the SPTM based on the Markov channel state model of order one as well as the measured PDFSD and can be described in four steps:

1) Assume that the channel enters state i at distance d.
2) Based on the PDFSD, generate the state duration Q_i of state i. The channel samples in the interval $[d, d + Q_i]$ are characterized by the fixed state i.
3) At time $d + Q_i + \Delta d$ the state i will change into state j, $j \neq i$, based on the state probability transition matrix.
4) We set $i = j$ and $d = d + Q_i + \Delta d$, and repeat the procedure starting from step 2).

Similar approach is mentioned in [12].

Due to equation (21) and the shape of $p_{BB}(Q)$ in Fig. 10 the PDFSD can be approximated by the piecewise exponential function as in Section III-D3.

V. The PDFSD Modeling for Multiple Satellite Systems

In order to achieve additional diversity gains, satellite constellations with multiple satellites in different orbital positions are used. The channels from simultaneously transmitting satellites are correlated to some extend, depending on the angular distance between satellite elevation angles [20]. Therefore, the LMS channel model should take into account the correlation between the satellites. For satellite systems consisting of more than one satellite, we define the state of the satellite system as the best

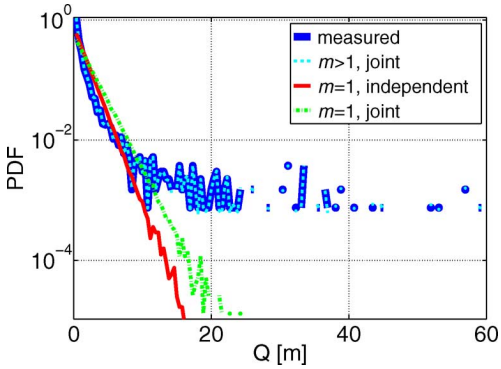

Fig. 13. Two satellite system. The PDF of the system blockage duration.

state out of all satellites (selection combining). Here, also Maximum Ratio Combining (MRC) can be considered due to better accuracy, but we assume here satellite selection combining due to its simplicity. Since the measurements from only two simultaneously transmitting satellites are available, we studied in detail the state modeling approach for the two satellite model in Section III, and based on these findings we propose in this section the modeling approach for multiple ($\geq$2) satellite systems.

If the satellite channel states had been modeled *independently* with an order $m = 1$ Markov state model, the PDF of the system blockage duration would not match the measurements as shown in Fig. 13. System blockages longer than 15 m can be hardly generated. If the satellite channel states had been modeled *independently* with dynamic higher order Markov state models, the system PDFSD would look close to the original PDFSD at lower blockage durations, but would not be able to match well the PDF for high blockage durations (we do not show this line in Fig. 13 in favor of better visibility). The long blockages are not very well matched due to the independence of the satellite states which leads to the maximum diversity gain, although that is hard to achieve in reality. In that case, the correlation between the states from different satellites is not captured.

Now we introduce a dynamic order joint Markov channel state model for multiple satellites in order to cope with this problem. In Section III we have introduced the Markov state joint model for two satellites and in Section IV we have introduced the dynamic SPTM model. Now we combine these two models. For multiple satellite systems, we describe the model by the system state probability transition tensor (SSPTT):

$$\boldsymbol{\mathcal{P}}^{\text{joint}}_{\text{trans}}(:,:,q) = \boldsymbol{P}^{\text{joint}}_{\text{trans}}(q\Delta d), \qquad q = 1, \ldots, q_{max}, \quad (25)$$

where $\boldsymbol{\mathcal{P}}^{\text{joint}}_{\text{trans}} \in \mathbb{R}_{+}^{M^a \times M^a \times q_{max}}$, M is the number of states per satellite, and a is the number of simultaneously active satellites. For satellite systems consisting of a simultaneously transmitting satellites, the stationary probabilities $P_{i_1 i_2 \ldots i_a}$ denote the probabilities that the system state is $i_1 i_2 \ldots i_a$. The system is in the state $i_1 i_2 \ldots i_a$ if the state of n-th satellite is i_n, $\forall n$ where $i_n \in \{\text{L}, \text{B}, \text{S}\}$ for the $M = 3$ case. The probabilities $P_{i_1 i_2 \ldots i_a}$ build the stationary state probability matrix $\boldsymbol{P} \in \mathbb{R}_{+}^{M \times M^{a-1}}$ and are estimated as

$$P_{i_1 i_2 \ldots i_a} = \frac{N_{i_1 i_2 \ldots i_a}}{N}, \quad (26)$$

where $N_{i_1 i_2 \ldots i_a}$ is the number of measurement samples corresponding to the state $P_{i_1 i_2 \ldots i_a}$ and N is the total number of considered measurement samples. The transition probabilities $p_{i_1 i_2 \ldots i_a j_1 j_2 \ldots j_a}(Q)$ between two consecutive time samples denote the probability of changing the system state from $i_1 i_2 \ldots i_a$ to $j_1 j_2 \ldots j_a$ given the current state duration Q of state $i_1 i_2 \ldots i_a$. The values $p_{i_1 i_2 \ldots i_a j_1 j_2 \ldots j_a}(Q)$ are estimated as

$$p_{i_1 i_2 \ldots i_a j_1 j_2 \ldots j_a}(Q) = \frac{N_{i_1 i_2 \ldots i_a j_1 j_2 \ldots j_a}(Q)}{N_{i_1 i_2 \ldots i_a}(Q)}, \quad (27)$$

where $N_{i_1 i_2 \ldots i_a j_1 j_2 \ldots j_a}(Q)$ is the number of transitions from state $i_1 i_2 \ldots i_a$ to $j_1 j_2 \ldots j_a$ and $N_{i_1 i_2 \ldots i_a}(Q)$ is the number of samples in state $i_1 i_2 \ldots i_a$, with the constraint that the current duration of the system state $i_1 i_2 \ldots i_a$ is Q. The number of states should be kept low enough since the number of transition probabilities in the system state probability transition matrix for one value of Q is equal to M^{2a}. Therefore, for systems with many satellites, only two states in the channel state model, namely the blocked and the LOS state, could be considered. Similarly as in the case of the one satellite model, this model has a dynamic order. The state sequence generation algorithm from $\boldsymbol{\mathcal{P}}^{\text{joint}}_{\text{trans}}$ is exactly the same as the corresponding algorithm for one satellite presented in Section IV-A. Generating the channel state sequence of two satellites jointly using this algorithm results in the PDF of the system blockage duration as depicted by a dashed light blue line in Fig. 13. It coincides with the measured system PDF of the blockage duration. In addition, this algorithm perfectly matches the duration of the shadowed as well as the LOS state and the PDF of the state duration of each satellite independently. This model is able to capture the state correlation between multiple satellites and generates a system channel state sequence with the same correlation properties.

To emphasize the need that the order of the joint Markov channel state model is dynamic, we plot in Fig. 13 also the PDF of the blockage for the joint Markov channel state model of order $m = 1$. The corresponding PDFSD of the generated state sequence represented by the dash-doted green curve is far away from the correct PDFSD.

A tradeoff between computational complexity of the model and performance has to be considered for systems with more than 5 satellites. As already stated, the number of transition probabilities in the system state probability transition matrix for one value of Q is equal to M^{2a}. Even if we reduce the number of states to $M = 2$ for $a = 5$ there are more than 1 000 elements in the SPTM that should be estimated as a function of the current state duration Q. This is not practical and demands a very large number of measured samples. For satellite systems with more than 5 satellites, an approximated model can be introduced. It focuses on perfect modeling of the system blockage which is the critical system state. Instead of estimating the whole STPM as a function of the current state duration, we only estimate one element in the STPM that corresponds to the system blockage (for a two satellite system it corresponds to the element p_{BBBB}) as a function of the current state duration Q. All the other transition elements in the corresponding STPM are scaled by using the constraint that the sum over each row in the STPM should be equal to 1. Such a model is able to model well only the PDF

of the system blockage duration and the mean state durations of each satellite independently, but that should be already enough to perform correct system planning with respect to the target system availability.

The PDFSD based channel state generation algorithm from Section IV-C can also be extended to multiple satellite systems: each system state can be defined by the permutations of states from different satellites. Then, the separate PDFSD is needed for each system state duration, where the number of system states grows exponentially with the number of satellites.

When the system state sequence generation is of major interest, we can first map the measured channel states from different satellites into the system state by using, for example, the satellite selection combining or MRC combining, followed by the models based on the state probability transition tensor for one satellite introduced in Section IV-A or on the PDFSD based modeling approach from Section IV-C. This approach gives a perfect match of the system state duration (it overlaps the dashed light blue line in Fig. 13) but is not able to generate the channel state sequence of each satellite separately and can be useful in the process of the system planning. This modeling approach can be very interesting for satellite systems with a large number of satellites, since the computational complexity of the model does not grow with the number of satellites.

VI. Conclusions

In this paper, we develop a satellite to outdoor channel model for satellite systems with one satellite and with multiple satellites based on measurements. We conclude that the Markov channel state model of fixed order is not able to generate the channel state sequence such that the generated PDFSD matches the measured PDFSD. Therefore, we introduce a dynamic higher order Markov state model for one satellite that can handle this problem, and we extend this model to multiple satellite systems. This approach models well the channel states of the whole system as well as the channel states of each satellite observed independently. It is able to capture the state correlation between two satellites and to transfer it into the generated system channel state sequence. We show that the proposed model can be approximated by a small set of parameters, which is useful for channel modeling purposes. In case of satellite systems with more than 5 satellites, the dynamic SPTM model can be computationally too complex. For such systems an approximate model is proposed. The statistical model describes the channel variations within each state: the PDF of the signal amplitude within each state is fitted to the Loo distribution. The PDF of the state duration is well approximated by piecewise exponential functions in all studied environments.

Appendix

Estimated Model Parameters

In this appendix we provide the numerical values of the estimated channel model parameters, namely the state probability matrix $\boldsymbol{P}$, the state transition probability matrix $\boldsymbol{P}_{\text{trans}}$, and Loo's model parameters μ, b_0, and d_0 for all four studied environments and both HEO and GEO satellite systems. GEO 1 and GEO 2 refer to the first and the second geostationary satellite, while HEO 1 and HEO 2 refer to the first and the second HEO satellite. Please note that in the matrix $\boldsymbol{P}$ the state where both satellites are blocked (double-blocked state) is in the upper left corner, while the state where both satellites are in the LOS state is in the lower right part. A similar notation is used for $\boldsymbol{P}_{\text{trans}}$: the transition probability from the double-blocked state to the double-blocked state is in the upper left part of $\boldsymbol{P}_{\text{trans}}$. Also note that the estimated state probability matrices and the estimated state transition matrices are not strictly symmetric due to the limited number of data samples.

A. Urban Environment

1) HEO:

$$\boldsymbol{P}=\begin{bmatrix} 0.02 & 0.02 & 0.18 \\ 0.02 & 0.02 & 0.16 \\ 00.04 & 0.04 & 0.50 \end{bmatrix}$$

$$\boldsymbol{P}_{\text{trans}}=\begin{bmatrix} 0.66 & 0.12 & 0 & 0.18 & 0.03 & 0 & 0.01 & 0 & 0 \\ 0.11 & 0.48 & 0.21 & 0.02 & 0.13 & 0.05 & 0 & 0 & 0 \\ 0 & 0.02 & 0.81 & 0 & 0.01 & 0.16 & 0 & 0 & 0 \\ 0.21 & 0.03 & 0 & 0.49 & 0.09 & 0 & 0.15 & 0.03 & 0 \\ 0.03 & 0.13 & 0.05 & 0.07 & 0.35 & 0.16 & 0.02 & 0.12 & 0.07 \\ 0 & 0.01 & 0.18 & 0 & 0.02 & 0.58 & 0 & 0.01 & 0.20 \\ 0 & 0 & 0 & 0.07 & 0.01 & 0 & 0.79 & 0.13 & 0 \\ 0 & 0 & 0 & 0.01 & 0.07 & 0.03 & 0.12 & 0.53 & 0.24 \\ 0 & 0 & 0 & 0 & 0 & 0.07 & 0 & 0.02 & 0.91 \end{bmatrix}$$

	$20\log_{10}(e^{\mu})$		$20\log_{10}(e^{\sqrt{d_0}})$		$10\log_{10}(2b_0)$	
	HEO 1	HEO 2	HEO 1	HEO 2	HEO 1	HEO 2
L	−0.5	−0.3	0.91	0.55	−16.7	−17.4
S	−5.2	−4.2	2.75	2.15	−14.4	−15.8
B	−13.1	−12.7	4.34	3.21	−24.2	−21.3

2) GEO:

$$\boldsymbol{P}=\begin{bmatrix} 0.22 & 0.06 & 0.05 \\ 0.09 & 0.05 & 0.04 \\ 0.10 & 0.18 & 0.21 \end{bmatrix}$$

$$\boldsymbol{P}_{\text{trans}}=\begin{bmatrix} 0.83 & 0.06 & 0 & 0.1 & 0.01 & 0 & 0 & 0 & 0 \\ 0.25 & 0.46 & 0.17 & 0.04 & 0.06 & 0.02 & 0 & 0 & 0 \\ 0 & 0.19 & 0.71 & 0 & 0.02 & 0.08 & 0 & 0 & 0 \\ 0.25 & 0.02 & 0 & 0.44 & 0.07 & 0 & 0.15 & 0.07 & 0 \\ 0.06 & 0.08 & 0.02 & 0.13 & 0.32 & 0.07 & 0.04 & 0.24 & 0.04 \\ 0 & 0.02 & 0.09 & 0 & 0.08 & 0.44 & 0 & 0.05 & 0.32 \\ 0 & 0 & 0 & 0.13 & 0.02 & 0 & 0.65 & 0.20 & 0 \\ 0 & 0 & 0 & 0.03 & 0.07 & 0.01 & 0.10 & 0.67 & 0.12 \\ 0 & 0 & 0 & 0 & 0.01 & 0.07 & 0 & 0.11 & 0.81 \end{bmatrix}$$

	$20\log_{10}(e^{\mu})$		$20\log_{10}(e^{\sqrt{d_0}})$		$10\log_{10}(2b_0)$	
	GEO 1	GEO 2	GEO 1	GEO 2	GEO 1	GEO 2
L	−1.2	−1.4	0.67	0.77	−14.7	−14.1
S	−4.3	−4.2	2.42	2	−16.9	−17.2
B	−16.5	−15.6	4.75	4.85	−18.5	−17.4

B. Suburban Environment With High Buildings

1) HEO:

$$\boldsymbol{P}=\begin{bmatrix}0 & 0 & 0.01\\ 0 & 0.02 & 0.03\\ 0.04 & 0.14 & 0.76\end{bmatrix}$$

$$\boldsymbol{P}_{\text{trans}}=\begin{bmatrix}0.11 & 0.19 & 0 & 0.11 & 0.5 & 0.03 & 0.03 & 0.03 & 0\\ 0.04 & 0.14 & 0.08 & 0.06 & 0.45 & 0.19 & 0 & 0.03 & 0.01\\ 0 & 0.04 & 0.25 & 0 & 0.12 & 0.52 & 0 & 0 & 0.07\\ 0.01 & 0.05 & 0 & 0.14 & 0.41 & 0.02 & 0.11 & 0.22 & 0.04\\ 0.01 & 0.06 & 0.02 & 0.07 & 0.32 & 0.13 & 0.05 & 0.26 & 0.08\\ 0 & 0.01 & 0.05 & 0 & 0.08 & 0.38 & 0 & 0.06 & 0.42\\ 0 & 0 & 0 & 0.01 & 0.02 & 0 & 0.47 & 0.47 & 0.03\\ 0 & 0 & 0 & 0.01 & 0.03 & 0.01 & 0.13 & 0.58 & 0.24\\ 0 & 0 & 0 & 0 & 0 & 0.01 & 0 & 0.05 & 0.94\end{bmatrix}$$

	$20\log_{10}(e^{\mu})$		$20\log_{10}(e^{\sqrt{d_0}})$		$10\log_{10}(2b_0)$	
	HEO 1	HEO 2	HEO 1	HEO 2	HEO 1	HEO 2
L	−0.6	−0.3	0.78	0.48	−17.1	−15.2
S	−4.3	−5.2	2.45	2.12	−16.8	−17.4
B	−11.9	−12.3	3.56	2.73	−20.2	−18.3

2) GEO:

$$\boldsymbol{P}=\begin{bmatrix}0.04 & 0.03 & 0.03\\ 0.06 & 0.07 & 0.05\\ 0.10 & 0.19 & 0.43\end{bmatrix}$$

$$\boldsymbol{P}_{\text{trans}}=\begin{bmatrix}0.58 & 0.11 & 0 & 0.21 & 0.08 & 0 & 0.01 & 0.01 & 0\\ 0.16 & 0.33 & 0.11 & 0.08 & 0.23 & 0.07 & 0 & 0.02 & 0\\ 0.01 & 0.15 & 0.510 & 0.01 & 0.09 & 0.23 & 0 & 0 & 0.01\\ 0.15 & 0.05 & 0 & 0.33 & 0.16 & 0.01 & 0.18 & 0.12 & 0\\ 0.05 & 0.11 & 0.03 & 0.13 & 0.32 & 0.09 & 0.07 & 0.16 & 0.04\\ 0 & 0.04 & 0.13 & 0.01 & 0.13 & 0.38 & 0 & 0.06 & 0.25\\ 0 & 0 & 0 & 0.10 & 0.05 & 0 & 0.55 & 0.30 & 0\\ 0 & 0 & 0 & 0.03 & 0.07 & 0.02 & 0.17 & 0.51 & 0.20\\ 0 & 0 & 0 & 0 & 0.01 & 0.03 & 0 & 0.08 & 0.88\end{bmatrix}$$

	$20\log_{10}(e^{\mu})$		$20\log_{10}(e^{\sqrt{d_0}})$		$10\log_{10}(2b_0)$	
	GEO 1	GEO 2	GEO 1	GEO 2	GEO 1	GEO 2
L	−1.1	−1.2	0.87	0.95	−16.5	−15.2
S	−5.2	−5.9	2.37	2.21	−17.3	−16.9
B	−14.7	−13.2	4.93	5.2	−17.7	−18.5

C. Suburban Environment With Low Buildings

1) HEO:

$$\boldsymbol{P}=\begin{bmatrix}0 & 0.01 & 0\\ 0 & 0 & 0.01\\ 0 & 0.02 & 0.96\end{bmatrix}$$

$$\boldsymbol{P}_{\text{trans}}=\begin{bmatrix}0 & 0.50 & 0 & 0.50 & 0 & 0 & 0 & 0 & 0\\ 0 & 0.07 & 0.06 & 0.07 & 0.36 & 0.42 & 0 & 0.02 & 0\\ 0 & 0 & 0 & 0 & 0.13 & 0.87 & 0 & 0 & 0\\ 0 & 0.04 & 0 & 0.17 & 0.36 & 0 & 0.17 & 0.26 & 0\\ 0.01 & 0.04 & 0.01 & 0.05 & 0.29 & 0.19 & 0.04 & 0.25 & 0.12\\ 0 & 0.02 & 0.04 & 0 & 0.03 & 0.45 & 0 & 0.03 & 0.43\\ 0 & 0 & 0 & 0.01 & 0.01 & 0.01 & 0.32 & 0.57 & 0.08\\ 0 & 0 & 0 & 0.01 & 0.02 & 0 & 0.10 & 0.58 & 0.29\\ 0 & 0 & 0 & 0 & 0 & 0 & 0.01 & 0.01 & 0.98\end{bmatrix}$$

	$20\log_{10}(e^{\mu})$		$20\log_{10}(e^{\sqrt{d_0}})$		$10\log_{10}(2b_0)$	
	HEO 1	HEO 2	HEO 1	HEO 2	HEO 1	HEO 2
L	−0.3	−0.5	0.37	0.57	−14.5	−16.9
S	−4.8	−5.6	1.62	2.3	−15.6	−16.5
B	−12.4	−11.7	2.45	2.13	−17.2	−18.4

2) GEO:

$$\boldsymbol{P}=\begin{bmatrix}0 & 0 & 0.01\\ 0 & 0.01 & 0.01\\ 0.01 & 0.07 & 0.89\end{bmatrix}$$

$$\boldsymbol{P}_{\text{trans}}=\begin{bmatrix}0.30 & 0.20 & 0.03 & 0.14 & 0.23 & 0.03 & 0.03 & 0.04 & 0\\ 0.02 & 0.48 & 0.20 & 0.05 & 0.13 & 0.08 & 0.01 & 0.02 & 0.01\\ 0 & 0.14 & 0.70 & 0.01 & 0.03 & 0.09 & 0 & 0.01 & 0.02\\ 0.07 & 0.03 & 0 & 0.23 & 0.28 & 0.02 & 0.13 & 0.24 & 0\\ 0.02 & 0.07 & 0.02 & 0.07 & 0.28 & 0.16 & 0.02 & 0.21 & 0.15\\ 0 & 0.01 & 0.04 & 0 & 0.08 & 0.44 & 0 & 0.03 & 0.40\\ 0 & 0 & 0 & 0.02 & 0.01 & 0 & 0.43 & 0.53 & 0.01\\ 0 & 0 & 0 & 0.01 & 0.02 & 0.01 & 0.09 & 0.54 & 0.33\\ 0 & 0 & 0 & 0 & 0 & 0.01 & 0 & 0.03 & 0.96\end{bmatrix}$$

	$20\log_{10}(e^{\mu})$		$20\log_{10}(e^{\sqrt{d_0}})$		$10\log_{10}(2b_0)$	
	GEO 1	GEO 2	GEO 1	GEO 2	GEO 1	GEO 2
L	−1.1	−1.3	0.54	0.87	−14.5	−14.1
S	−4.5	−4.2	1.72	1.95	−16.1	−16.5
B	−14.8	−14.6	3.88	3.4	−20.5	−20.1

D. Rural Environment

1) HEO:

$$\boldsymbol{P}=\begin{bmatrix}0 & 0 & 0\\ 0 & 0.04 & 0.03\\ 0 & 0.03 & 0.90\end{bmatrix}$$

$$\boldsymbol{P}_{\text{trans}}=\begin{bmatrix}0 & 0 & 0 & 0.50 & 0 & 0.50 & 0 & 0 & 0\\ 0 & 0 & 0 & 0 & 1 & 0 & 0 & 0 & 0\\ 0 & 0 & 0.36 & 0 & 0.01 & 0.53 & 0 & 0 & 0.10\\ 0 & 0.01 & 0 & 0.14 & 0.61 & 0.03 & 0.02 & 0.17 & 0.02\\ 0 & 0 & 0 & 0.07 & 0.56 & 0.17 & 0.02 & 0.13 & 0.05\\ 0 & 0 & 0.04 & 0 & 0.16 & 0.49 & 0 & 0.04 & 0.27\\ 0 & 0 & 0 & 0.03 & 0.21 & 0.01 & 0.13 & 0.58 & 0.04\\ 0 & 0 & 0 & 0.02 & 0.18 & 0.06 & 0.05 & 0.53 & 0.16\\ 0 & 0 & 0 & 0 & 0 & 0.01 & 0 & 0.01 & 0.98\end{bmatrix}$$

	$20\log_{10}(e^{\mu})$		$20\log_{10}(e^{\sqrt{d_0}})$		$10\log_{10}(2b_0)$	
	HEO 1	HEO 2	HEO 1	HEO 2	HEO 1	HEO 2
L	−0.4	−0.3	0.44	0.61	−15.2	−17.3
S	−4.1	−4.4	1.51	2.46	−16.1	−17.7
B	−12.4	−11.8	1.72	2.3	−23.8	−22.2

2) GEO:

$$\boldsymbol{P}=\begin{bmatrix}0.01 & 0.02 & 0.01\\ 0.03 & 0.06 & 0.04\\ 0.03 & 0.09 & 0.71\end{bmatrix}$$

$$\boldsymbol{P}_{\text{trans}}=\begin{bmatrix}0.26 & 0.17 & 0.01 & 0.25 & 0.24 & 0.02 & 0.01 & 0.03 & 0.01\\ 0.10 & 0.24 & 0.07 & 0.12 & 0.35 & 0.09 & 0.01 & 0.02 & 0\\ 0.01 & 0.11 & 0.36 & 0.01 & 0.13 & 0.35 & 0 & 0.01 & 0.02\\ 0.09 & 0.08 & 0 & 0.32 & 0.30 & 0.02 & 0.08 & 0.09 & 0.02\\ 0.04 & 0.10 & 0.03 & 0.15 & 0.37 & 0.11 & 0.04 & 0.13 & 0.04\\ 0 & 0.04 & 0.10 & 0.01 & 0.15 & 0.46 & 0 & 0.04 & 0.20\\ 0 & 0.01 & 0 & 0.10 & 0.09 & 0 & 0.35 & 0.43 & 0.02\\ 0 & 0 & 0 & 0.03 & 0.07 & 0.02 & 0.12 & 0.53 & 0.23\\ 0 & 0 & 0 & 0 & 0 & 0.01 & 0 & 0.03 & 0.96\end{bmatrix}$$

	$20\log_{10}(e^{\mu})$		$20\log_{10}(e^{\sqrt{d_0}})$		$10\log_{10}(2b_0)$	
	GEO 1	GEO 2	GEO 1	GEO 2	GEO 1	GEO 2
L	−1.1	−1.3	0.47	0.67	−14.3	−13.2
S	−4.1	−4.5	1.73	1.61	−15.2	−15.9
B	−15.8	−15.6	2.06	2.3	−18.1	−18.7

REFERENCES

[1] B. Vucetic and J. Du, "Channel modeling and simulation in satellite mobile communication systems," *IEEE Journal on Selected Areas in Communications*, vol. 10, no. 8, Oct. 1992.

[2] C. Loo, "A statistical model for a land mobile satellite link," *IEEE Trans. Vehicular Technology*, vol. 34, pp. 122–127, Aug. 1985.

[3] A. Abdi, W. C. Lau, M.-S. Alouini, and M. Kaveh, "A new simple model for land mobile satellite channels: First- and second-order statistics," *IEEE Trans. Wireless Communications*, vol. 2, pp. 519–528, May 2003.

[4] H. Suzuki, "A statistical model for urban radio propagation," *IEEE Trans. Communications*, vol. 25, pp. 673–680, Jul. 1977.

[5] E. Lutz, D. Cygan, M. Dippold, F. Dolainsky, and W. Papke, "The land mobile satellite communication channel-recording, statistics, and channel model," *IEEE Trans. Vehicular Technology*, vol. 40, pp. 375–386, May 1991.

[6] E. Lutz, "A Markov model for correlated land mobile satellite channels," *International Journal of Satellite Communications*, vol. 14, pp. 333–339, 1996.

[7] F. P. Fontán, J. P. González, M. J. S. Ferreiro, M. A. V. Castro, S. Buonomo, and J. P. Baptista, "Complex envelope three-state Markov model based simulator for the narrow-band LMS channel," *International Journal of Satellite Communications*, vol. 15, pp. 1–15, 1997.

[8] F. P. Fontán, M. A. V. Castro, S. Buonomo, J. P. Baptista, and B. Rastburg, "S-band LMS propagation channel behaviour for different environments, degrees of shadowing and elevations angles," *IEEE Trans. Broadcasting*, vol. 44, no. 1, Mar. 1998.

[9] F. P. Fontán, M. V. Castro, C. E. Cabado, J. P. García, and E. Kubista, "Statistical modeling of the LMS channel," *IEEE Trans. Vehicular Technology*, vol. 50, no. 6, Nov. 2001.

[10] A. Jahn, "Propagation characteristics for land mobile satellite systems from L-band to EHF-band," *European Trans. Telecommun.*, vol. 19, May 2001.

[11] L. Husson, A. Beffani, J.-C. Dany, and M. Pourmir, "Extraction of empirical models from experimental measurements in the L-band for mobile satellite transmissions," in *Proc. 19th American Institute of Aeronautics and Astronautics: International Communications Satellite Systems Conference (AIAA ICSSC)*, Toulouse, France, Apr. 2001.

[12] L. E. Bråten and T. Tjelta, "Semi-Markov multistate modeling of the land mobile propagation channel for geostationary satellites," *IEEE Trans. Antennas and Propagation*, vol. 50, no. 12, pp. 1795–1802, Dec. 2002.

[13] S. Scalise, C. Alasseur, L. Husson, and H. Ernst, "Accurate and novel modeling of the land mobile satellite channel using reversible jump Markov chain Monte Carlo technique," in *Proc. Global Telecommunications Conference (GLOBECOM)*, San Francisco, USA, Nov. 2006.

[14] C. Alasseur, S. Scalise, L. Husson, and H. Ernst, "A novel approach to model the land mobile satellite channel through reversible jump Markov chain Monte Carlo technique," *IEEE Trans. Wireless Communications*, vol. 7, no. 2, pp. 532–542, Feb. 2008.

[15] L. Rabiner, "A tutorial on hidden Markov models and selected applications in speech recognition," *Proceedings of the IEEE*, vol. 77, pp. 257–286, Feb. 1989.

[16] A. Heuberger, "Fade correlation and diversity effects in satellite broadcasting to mobile users in S-band," *International Journal of Satellite Communications and Networking*, Jun. 2008.

[17] R. A. Michalski, *An Overview of the XM Satellite Radio System*. Washington, DC: Published by American Institute of Aeronautics and Astronautics, 2002.

[18] D. H. Layer, "Digital radio takes to the road," *IEEE Spectrum*, 2001.

[19] M. Richharia, *Mobile Satellite Communications, Principles and Trends*. Great Britain: Pearson Education Limited, 2001.

[20] *"Handbook of Propagation Effects for Vehicular and Personal Mobile Satellite Systems,"* John Hopkins University, University of Texas, Austin, USA, 1998.

Marko Milojević (S'07) was born in Belgrade on June 5, 1977. He received the Dipl.-Ing. degree in telecommunications engineering at Faculty of Electrical Engineering, Belgrade, Serbia in 2001. Afterwards he joined the Communications Research Laboratory at Ilmenau University of Technology, Ilmenau, Germany, where he works as a research assistant. His research interests include channel modeling for wireless communications, array signal processing and multi-dimensional linear algebra. He is currently pursuing his Ph.D. at Ilmenau University of Technology.

Martin Haardt (S'90–M'98–SM'99) has been a Full Professor in the Department of Electrical Engineering and Information Technology and Head of the Communications Research Laboratory at Ilmenau University of Technology, Germany, since 2001.

After studying electrical engineering at the Rohr-University Bottom, Germany, and at Prude University, USA, he received his Diplom-Ingenieur (M.S.) degree from the Ruhr-University Bochum in 1991 and his Doktor-Ingenieur (Ph.D.) degree from Munich University of Technology in 1996.

In 1997, he joined Siemens Mobile Networks in Munich, Germany, where he was responsible for strategic research for third generation mobile radio systems. From 1998 to 2001 he was the Director for International Projects and University Cooperations in the mobile infrastructure business of Siemens in Munich, where his work focused on mobile communications beyond the third generation. During his time at Siemens, he also taught in the international Master of Science in Communications Engineering program at Munich University of Technology. He received the Vodafone (formerly Mannesmann Mobilfunk) Innovations-Award for outstanding research in mobile communications, the ITG best paper award from the Association of Electrical Engineering, Electronics, and Information Technology (VDE), and the Rohde & Schwarz Outstanding Dissertation Award. In the fall of 2006 and the fall of 2007 he was a visiting professor at the University of Nice in Sophia-Antipolis, France, and at the University of York, United Kingdom, respectively. His research interests include wireless communications, array signal processing, high-resolution parameter estimation, as well as numerical linear and multi-linear algebra. Prof. Haardt has served as an Associate Editor for the IEEE TRANSACTIONS ON SIGNAL PROCESSING (2002–2006), the IEEE SIGNAL PROCESSING LETTERS (since 2006), the Research Letters in Signal Processing (since 2007), and the Hindawi Journal of Electrical and Computer Engineering (since 2009). He also served as the technical co-chair of the IEEE International Symposiums on Personal Indoor and Mobile Radio Communications (PIMRC) 2005 in Berlin, Germany.

Ernst Eberlein is head of department digital communication at Fraunhofer-Institute for Integrated Circuits IIS. He finished his studies of electrical engineering at the Friedrich-Alexander University Erlangen-Nuremberg end 1984 and joint Fraunhofer IIS in 1985. Until 1995, his main focus was on DSP based systems for audio and multimedia applications. The team was responsible for the development of MP3 including algorithm development, standardization and prototyping. Since 1995, Ernst Eberlein's focus is more on digital communication systems. This includes major contributions to satellite-based broadcasting systems for mobile reception including complementary ground components. From 1995 to 1997, he was in charge of the receiver development for the WorldSpace system. In the years 1997 to 1999 he was responsible for the XM satellite radio system development and validation at Fraunhofer IIS. Since 2001 Ernst Eberlein is responsible for the coordination of the research activities in the area of digital communication.

Albert Heuberger (M'97) finished his studies of electrical engineering at the Friedrich-Alexander University Erlangen-Nuremberg in 1987 and his Ph.D. from the same university in 2005. He joined the Fraunhofer-Institute for Integrated Circuits IIS in 1987 and worked as head of the communication systems department until May 2008. In this position he was responsible for contract research for digital broadcasting transmission. Since June 2008, he has been full professor at the Ilmenau University of Technology and head of the Digital Broadcasting Research Laboratory as well as head of the Fraunhofer research group for Digital Broadcasting. His research interests are transmission systems for digital broadcasting applications with focus on channel modeling and QoS prediction for satellite and terrestrial broadcasting systems. He is also giving lectures at the University of Erlangen-Nuremberg and the German University in Cairo.